AIP | Journal of Applied Physics

Pressure and electric field effects on piezoelectric responses of KNbO3

Linyun Liang, Y. L. Li, Fei Xue, and Long-Qing Chen

Citation: J. Appl. Phys. **112**, 064106 (2012); doi: 10.1063/1.4752418
View online: http://dx.doi.org/10.1063/1.4752418
View Table of Contents: http://jap.aip.org/resource/1/JAPIAU/v112/i6
Published by the American Institute of Physics.

Related Articles

Positive effective Q12 electrostrictive coefficient in perovskites
J. Appl. Phys. 112, 094106 (2012)

Large and temperature-independent piezoelectric response in Pb(Mg1/3Nb2/3)O3-BaTiO3-PbTiO3
Appl. Phys. Lett. 101, 192901 (2012)

Piezoelectric nonlinearity and frequency dispersion of the direct piezoelectric response of BiFeO3 ceramics
J. Appl. Phys. 112, 064114 (2012)

Structure and properties of La-modified Na0.5Bi0.5TiO3 at ambient and elevated temperatures
J. Appl. Phys. 112, 054111 (2012)

Modeling of dielectric and piezoelectric response of 1-3 type piezocomposites
J. Appl. Phys. 112, 044107 (2012)

Additional information on J. Appl. Phys.

Journal Homepage: http://jap.aip.org/
Journal Information: http://jap.aip.org/about/about_the_journal
Top downloads: http://jap.aip.org/features/most_downloaded
Information for Authors: http://jap.aip.org/authors

ADVERTISEMENT

Downloaded 13 Nov 2012 to 146.186.211.66. Redistribution subject to AIP license or copyright; see http://jap.aip.org/about/rights_and_permissions

Pressure and electric field effects on piezoelectric responses of $KNbO_3$

Linyun Liang,[1,a)] Y. L. Li,[2] Fei Xue,[1] and Long-Qing Chen[1]
[1]*Department of Materials Science & Engineering, The Pennsylvania State University, Pennsylvania 16802, USA*
[2]*Pacific Northwest National Laboratory, Richland, Washington 99352, USA*

(Received 15 May 2012; accepted 15 August 2012; published online 18 September 2012)

The dielectric and piezoelectric properties of a $KNbO_3$ single crystal under applied hydrostatic pressure and positive bias electric field are investigated using phenomenological Landau-Ginzburg-Devonshire thermodynamic theory. It is shown that the hydrostatic pressure effect on the dielectric and piezoelectric properties is similar to temperature, suggesting a common underlying mechanism for the piezoelectric anisotropy and its enhancement. The stable phase diagram of $KNbO_3$ as a function of temperature and positive bias electric field is constructed. The maximum piezoelectric coefficient d_{33}^{o*} varying with temperature and electric field is calculated. © *2012 American Institute of Physics*. [http://dx.doi.org/10.1063/1.4752418]

Much attention has been paid to environmental preservation worldwide in recent years. In the research field of piezoelectric ceramics, there is an increasing strong demand to develop alternative lead-free piezoelectric materials against PZT based compounds, which are being widely used in various fields as the most important piezoelectric materials. Potassium niobate, $KNbO_3$ is one of the important candidates of lead-free piezoelectric materials since the single crystals show a large electromechanical coupling factor and the high Curie point.[1–4] Although the $KNbO_3$ has good piezoelectricity, piezoelectric coefficients of $KNbO_3$ are much lower than those of PZT based materials. Various experimental approaches have been explored to improve the piezoelectric responses including applied external fields,[4,5] chemical etching,[3] domain engineering,[6] etc. However, so far, no significant improvement has been achieved.

In understanding of mechanisms of the piezoelectric coupling in ferroelectric piezoelectrics, most of the progresses have been centered on the discovery of the enhanced piezoelectric responses along nonpolar directions. Large piezoelectric responses along nonpolar crystallographic directions were reported in both complex relaxors[7–9] and simple perovskites[3,10] in the past years. The origin of such enhancement of piezoelectric response in perovskites has been explained using a polarization rotation mechanism based on first-principle calculations[11–13] and free-energy flattening mechanism based on a phenomenological thermodynamic analysis.[14,15] Based on the thermodynamic analysis, the effects of electric field, composition, stress and temperature on the piezoelectric properties of $BaTiO_3$, $PbTiO_3$, and PZT perovskite crystals have been examined using the Landau-Ginzburg-Devonshire (LGD) thermodynamic theory.[16–20] It is shown that the application of external fields enhances piezoelectric coefficients along the nonpolar directions, which is related to the phase transitions that are accompanied by huge shear piezoelectric coefficients, resulting an enhancement of longitudinal piezoelectric coefficient $d_{33}^*(\theta, \phi, \psi)$. For the tetragonal $BaTiO_3$ single crystal, a higher piezoelectric response was observed along no-polar [111].[10] While in the orthorhombic phase, the highest piezoelectric responses with d_{33} over 500 pC/N were observed when an electric field was applied along [001] no-polar direction.[21] It is well known that $KNbO_3$ crystals exhibit a series of transitions similar to $BaTiO_3$ with cooling from Curie temperature but the stable phase is orthorhombic at room temperature. It is expected that $KNbO_3$ crystals may have similar enhancement of piezoelectric response under external fields. Room temperature piezoelectric coefficients of $KNbO_3$ have been well determined experimentally in the earlier studies.[22–25] Wada *et al.*[4] investigated the piezoelectric properties of $KNbO_3$ crystals along the polar $[110]_c$ direction and $[001]_c$ of engineered domain direction. In their following work, they have obtained all piezoelectric coefficients based on the single-domain crystals.[6] In our previous work, we calculated a set of piezoelectric coefficients as a function of crystallographic orientation and temperature,[26] and also the piezoelectric coefficients along the applied electric field directions.[27] However, theoretical analysis of the crystallographic orientation dependence of piezoelectric coefficients of $KNbO_3$ single crystals under the application of electric fields and hydrostatic pressure has not been studied. Thus, the objective of this paper is to study the hydrostatic pressure and electric field effect on the dielectric and piezoelectric responses of single-domain $KNbO_3$ crystals using the LGD theory.

Under external pressure and electric fields, the LGD free energy can be written as[28]

[a)]Author to whom correspondence should be addressed. Electronic mail: lul22@psu.edu.

 © 2012 American Institute of Physics

Downloaded 13 Nov 2012 to 146.186.211.66. Redistribution subject to AIP license or copyright; see http://jap.aip.org/about/rights_and_permissions

$$
\begin{aligned}
f_{LGD}(P_i,\sigma,E_i) &= \alpha_1(P_1^2+P_2^2+P_3^2)+\alpha_{11}(P_1^4+P_2^4+P_3^4)+\alpha_{12}(P_1^2P_2^2+P_2^2P_3^2+P_1^2P_3^2)\\
&+\alpha_{111}(P_1^6+P_2^6+P_3^6)+\alpha_{112}[P_1^4(P_2^2+P_3^2)+P_2^4(P_1^2+P_3^2)+P_3^4(P_1^2+P_2^2)]\\
&+\alpha_{123}P_1^2P_2^2P_3^2+\alpha_{1111}(P_1^8+P_2^8+P_3^8)+\alpha_{1112}[P_1^6(P_2^2+P_3^2)+P_2^6(P_1^2+P_3^2)+P_3^6(P_1^2+P_2^2)]\\
&+\alpha_{1122}(P_1^4P_2^4+P_2^4P_3^4+P_1^4P_3^4)+\alpha_{1123}(P_1^4P_2^2P_3^2+P_2^4P_3^2P_1^2+P_3^4P_1^2P_2^2)\\
&-\frac{1}{2}s_{11}(\sigma_1^2+\sigma_2^2+\sigma_3^2)-s_{12}(\sigma_1\sigma_2+\sigma_2\sigma_3+\sigma_3\sigma_1)-\frac{1}{2}s_{44}(\sigma_4^2+\sigma_5^2+\sigma_6^2)\\
&-Q_{11}(\sigma_1P_1^2+\sigma_2P_2^2+\sigma_3P_3^2)-Q_{12}[\sigma_1(P_2^2+P_3^2)+\sigma_2(P_1^2+P_3^2)+\sigma_3(P_1^2+P_2^2)]\\
&-Q_{44}[\sigma_4P_2P_3+\sigma_5P_1P_3+\sigma_6P_1P_2)]-E_1P_1-E_2P_2-E_3P_3,
\end{aligned}
\tag{1}
$$

where α with subscript index represents expansion coefficient under zero stress, s_{ij} is elastic compliance at constant polarization P_i, Q_{ij} is electrostrictive coefficient, σ_i and E_i are stress and electric field. The values of α_{ij}, s_{ij}, and Q_{ij} are taken form Ref. 29.

We use the superscript 'p' with $p=c, t, o, r$ to indicate the physical quantities measured in the cubic, tetragonal, orthorhombic, and rhombohedral crystallographic coordinate systems, respectively. The dielectric stiffness coefficient χ_{ij}^c is obtained via $\chi_{ij}^c=\varepsilon_0\partial^2 f_{LGD}/\partial P_i\partial P_j$.[28] The dielectric susceptibility η_{ij}^c can be determined from the reciprocal of χ_{ij}^c using $\eta_{ij}^c=A_{ji}/\Delta$, where A_{ji} and Δ are the cofactor and determinant of the χ_{ij}^c matrix. For the stable orthorhombic phase at room temperature, we rotate the cubic coordinate system into a new coordinate system defined by $[100]^o=[100]^c$, $[010]^o=[01\bar{1}]^c$, and $[001]^o=[011]^c$. The dielectric susceptibility η_{ij}^o in the new coordinate system can be simply obtained by $\eta_{ij}^o=1/\chi_{ij}^o$ due to the diagonalized matrix of dielectric stiffness coefficient χ_{ij}^o. The relationship of the dielectric stiffness coefficients between the old and new coordinate systems is given by, $\chi_{11}^o=\chi_{11}^c$, $\chi_{22}^o=\chi_{33}^c-\chi_{23}^c$, $\chi_{33}^o=\chi_{33}^c+\chi_{23}^c$, and $\chi_{12}^o=\chi_{13}^o=\chi_{23}^o=0$.[28] Therefore, the piezoelectric coefficients in the orthorhombic phase depending on the dielectric susceptibilities and polarizations in the rotated system are given by

$$
\begin{aligned}
d_{15}^o &= \varepsilon_0\eta_{11}^o(\sigma_i,E_i)Q_{44}P_3^o(\sigma_i,E_i),\\
d_{24}^o &= 2\varepsilon_0\eta_{22}^o(\sigma_i,E_i)[Q_{11}-Q_{12}]P_3^o(\sigma_i,E_i),\\
d_{31}^o &= 2\varepsilon_0\eta_{33}^o(\sigma_i,E_i)Q_{12}P_3^o(\sigma_i,E_i),\\
d_{32}^o &= \frac{1}{2}\varepsilon_0\eta_{33}^o(\sigma_i,E_i)[2Q_{11}+2Q_{12}-Q_{44}]P_3^o(\sigma_i,E_i),\\
d_{33}^o &= \frac{1}{2}\varepsilon_0\eta_{33}^o(\sigma_i,E_i)[2Q_{11}+2Q_{12}+Q_{44}]P_3^o(\sigma_i,E_i),
\end{aligned}
\tag{2}
$$

where η_{ij}^o is related to the dielectric coefficient ε_{ij}^o by a relation of $\eta_{ij}^o\approx 1+\eta_{ij}^o=\varepsilon_{ij}^o$.

The orientation dependence of the longitudinal piezoelectric coefficient d_{33}^{o*} in the orthorhombic $KNbO_3$ crystal under hydrostatic pressure and electric field can be calculated by[26]

$$
\begin{aligned}
d_{33}^{o*}(\theta,\phi) &= (d_{15}^o(\sigma_i,E_i)+d_{31}^o(\sigma_i,E_i))\cos\theta\sin^2\theta\sin^2\phi\\
&+\left(d_{24}^o(\sigma_i,E_i)+d_{32}^o(\sigma_i,E_i)\right)\cos\theta\sin^2\theta\cos^2\phi\\
&+d_{33}^o(\sigma_i,E_i)\cos^3\theta,
\end{aligned}
\tag{3}
$$

where the Euler angle ϕ describes the rotation around the $[001]^o=[011]^c$ axis, and θ describes the rotation away from the $[001]^o$ axis around the rotated $[100]^o$ axis. $\phi=\pi/2$ and $\theta=\arcsin(1/\sqrt{3})$ correspond to the coordinates associated with the rhombohedral phase while $\phi=0$ and $\theta=-\pi/4$ are associated with the tetragonal phase. The other set of piezoelectric coefficients in different ferroelectric phases under the applied external fields can be obtained in a similar way.

We first consider the effects of hydrostatic pressure on the dielectric and piezoelectric responses of orthorhombic $KNbO_3$. The hydrostatic pressure is expressed by $\sigma_1=\sigma_2=\sigma_3=-\sigma, \sigma_4=\sigma_5=\sigma_6=0$. It alters the phase transition temperature. A phase diagram as a function of hydrostatic pressure σ and temperature T has been constructed elsewhere.[29] Based on this thermodynamic phase diagram, the pressure dependencies of dielectric susceptibilities and piezoelectric coefficients at two chosen temperatures $T=25\,^\circ$C and $100\,^\circ$C for the orthorhombic phase are presented in Fig. 1. It should be noted that the applied pressure range is different for the two different temperatures since the phase transition-pressure is different based on the thermodynamic diagram. It is seen that the dielectric susceptibilities η_{11}^o and η_{22}^o which are perpendicular to the polarization direction $[001]^o$. are sensitive to the pressure. η_{11}^o decreases and η_{22}^o increases with the pressure. η_{33}^o is relatively insensitive to the pressure. Correspondingly, we can easily see from Eq. (2) that the piezoelectric coefficients d_{15}^o ($\propto\eta_{11}^o$) and d_{24}^o($\propto\eta_{22}^o$) change significantly with the pressure while d_{31}^o, d_{32}^o, and d_{33}^o($\propto\eta_{33}^o$) change slightly (the value of d_{31}^o is close to d_{32}^o but not plotted in Fig. 2 for the sake of clarity). The large enhancement of the shear piezoelectric coefficients d_{24}^o is ascribed to the ferroelectric phase transition from the applied hydrostatic pressure. Their change with the pressure will result in strong anisotropy of d_{33}^{o*}. In order to illustrate the crystallographic orientation dependence of d_{33}^{o*}, the d_{33}^{o*} surface as a function of pressure at room temperature is plotted in Fig. 2. We analyzed the piezoelectric responses on the $(010)^o$ and $(100)^o$ planes which are corresponding to $\phi=90^\circ$ and $\phi=0^\circ$, respectively. At room temperature, the piezoelectric coefficient d_{33}^{o*} as a function of angle θ with various pressures in different planes is given in Fig. 3. It is seen that when $\phi=90^\circ$, the maximum of d_{33}^{o*} decreases with increasing pressure and its corresponding angle θ_{max} reduces rapidly from 52.0° at 0 GPa to 14.6° at 6 GPa. The hydrostatic pressure tends to rotate the direction of maximum d_{33}^{o*} into the $[001]^o$ direction. On the other hand, for $\phi=0^\circ$, d_{33}^{o*} increases significantly while θ_{max} increases slightly with pressure. For example, d_{33max}^{o*} is 100.9 pC/N

Downloaded 13 Nov 2012 to 146.186.211.66. Redistribution subject to AIP license or copyright; see http://jap.aip.org/about/rights_and_permissions

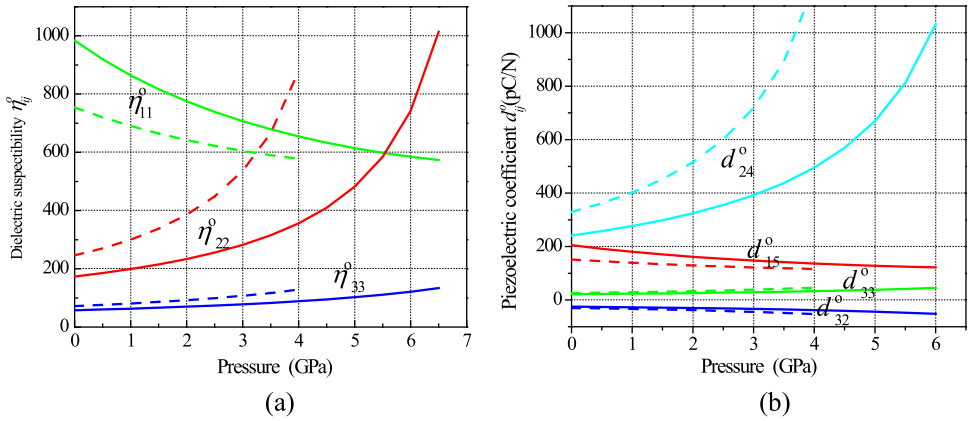

FIG. 1. The hydrostatic pressure dependence of (a) dielectric susceptibilities and (b) piezoelectric coefficients of $KNbO_3$ at 25 °C (solid line) and 100 °C (dashed line).

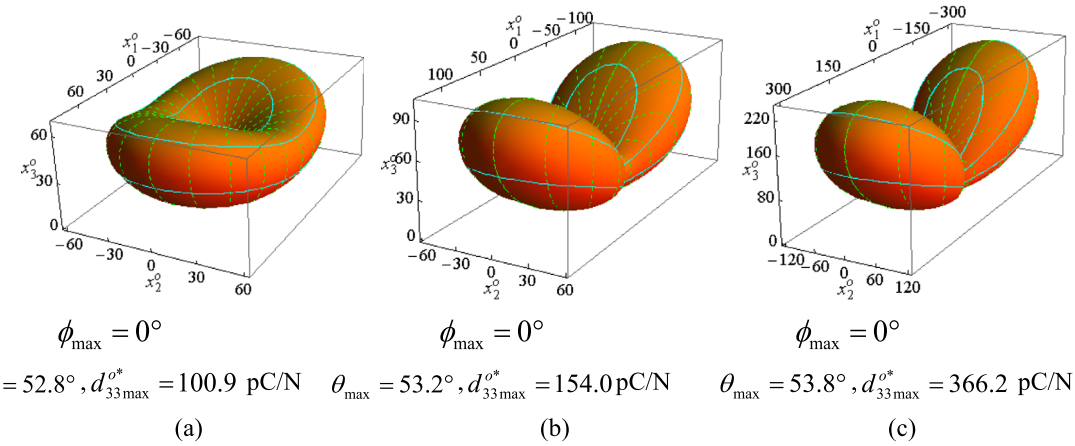

FIG. 2. At room temperature, the orientation dependence of piezoelectric coefficient d^{o*}_{33} under three selected pressures, (a) $\sigma = 0$ GPa; (b) $\sigma = 3$ GPa; (c) $\sigma = 6$ GPa. Angles ϕ_{max} and θ_{max} at which the maximum of d^{o*}_{33} occurs are indicated for each pressure. The three coordinate axes correspond to $x^o_1 = d^{o*}_{33}\sin\theta\cos\phi$, $x^o_2 = d^{o*}_{33}\sin\theta\sin\phi$, $x^o_3 = d^{o*}_{33}\cos\theta$, respectively. The numerical values marked on the axes have unit pC/N. The piezoelectric coefficients are symmetry with respective to the plane of $x^o_3 = 0$, so only the upper half of the coordinate space is shown.

without applied pressure and then increases to 366.2 pC/N at 6 GPa. d^{o*}_{33max} for $\phi = 0°$ is nearly nine times larger than that of $\phi = 90°$ at 6 GPa. The largest d^{o*}_{33max} always lies in the $(100)^o$ plane ($\phi = 0°$) in the orthorhombic stable phase.

As seen from Eq. (3) and Fig. 1, d^{o*}_{33} is dominated by d^o_{24} when close to the orthorhombic-tetragonal phase transition temperatures. The shear piezoelectric coefficients d^o_{15} and d^o_{24} are related to the permittivities perpendicular to the direction of the spontaneous polarization axis $[001]^o$. It is known that the significant enhancement of d^o_{15} and d^o_{24} is directly related to the presence of the orthorhombic-rhombohedral or tetragonal-orthorhombic phase transitions. Therefore, the largest d^{o*}_{33} along $(100)^o$ plane at high pressure implies that d^o_{24} dominate d^{o*}_{33} and the tetragonal-orthorhombic phase transition has a stronger effect on d^{o*}_{33}.

The pressure dependencies of the dielectric susceptibility for the orthorhombic phase can be understood from the pressure dependence of its free energy profile (Fig. 4). The free energy of the orthorhombic phase at a given pressure as a function of polarization can be obtained through assuming the polarization $P_1 = 0$ and $P_2 = P_3 = \sqrt{2}P_S$. The flattening of the free energy profile implies an increase of the system's

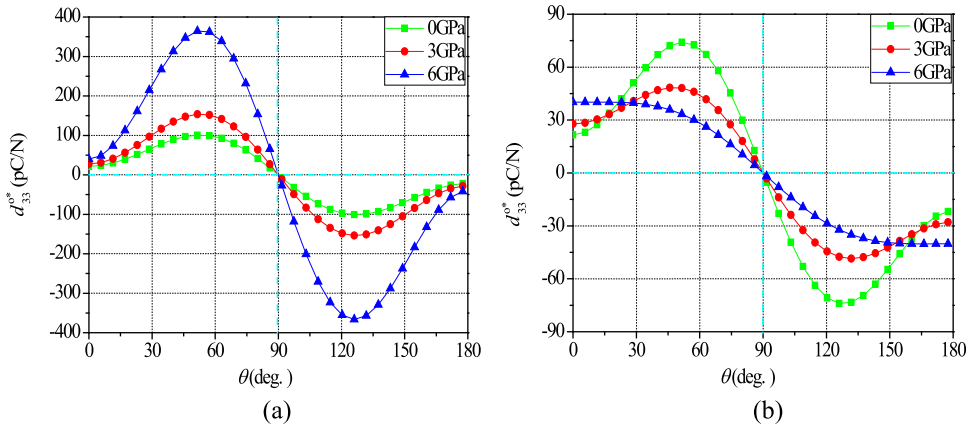

FIG. 3. Room temperature piezoelectric coefficient d^{o*}_{33} in the orthorhombic $KNbO_3$ as a function of angle θ at various pressures in different planes, (a) $\phi = 0°$ and (b) $\phi = 90°$.

Downloaded 13 Nov 2012 to 146.186.211.66. Redistribution subject to AIP license or copyright; see http://jap.aip.org/about/rights_and_permissions

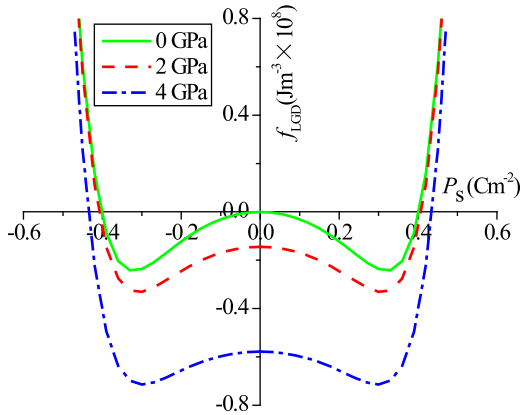

FIG. 4. A calculated free energy as a function of polarization (P_s) under various selected pressures in the orthorhombic phase at room temperature.

dielectric susceptibility, and thus the increase of its piezoelectric response, i.e., a dielectric softening of the crystal along the polar directions. It is noted that the flattening of free energy under a pressure becomes more prominent near a phase transition.

Next, we calculate the piezoelectric responses of $KNbO_3$ crystal under applied electric field. In order to find the stable ferroelectric phase with the applied electric field, a phase diagram as a function of temperature and electric field is constructed and given in Fig. 5.

From the temperature-electric field phase diagrams, it is seen that the applied electric field could induce ferroelectric phases other than the regular tetragonal phase ($P_1 = P_2 = 0$, $P_3 > 0$), orthorhombic phase ($P_1 = 0$, $P_2 = P_3 > 0$), and rhombohedral phase ($P_1 = P_2 = P_3 > 0$). For the sake of simplicity, here we only focus on the dielectric susceptibilities η^o_{ij} and piezoelectric coefficients d^o_{ij} at the chosen two temperatures 200 °C and −45 °C for an applied field along the polar direction ($E_{[011]^c}$) where there is only the regular orthorhombic phase. The calculated dielectric susceptibilities and piezoelectric coefficients are shown in Fig. 6. It is easily seen that a positive bias field reduces the dielectric susceptibilities and piezoelectric coefficients. Of particular interest are the temperature regimes close to two adjacent phase transitions at the small electric field, i.e., from the orthorhombic phase to high-temperature phase α [defined by $P_3 > P_2$, $P_1 = 0$ in Fig. 5(b)] and from the orthorhombic phase to low-temperature phase β [defined by $P_2 = P_3 > P_1 > 0$ in Fig. 5(b)]. For example, at 200 °C close to the orthorhombic-α phase transition, the positive bias field reduces η^o_{22}, and consequently, leads to a low d^o_{24} [see Fig. 6 and Eq. (2)]. If the temperature decreases to −45 °C which is close to the orthorhombic-β phase transition at small applied electric field $E_{[011]^c}$, a similar trend for η^o_{11} was observed but with a low d^o_{15} [see Fig. 7 and Eq. (2)]. In generally speaking, at high temperatures, d^o_{24} is relatively large, while at lower temperatures, d^o_{15} becomes larger than d^o_{24} [Fig. 6(b)]. It is known that the significant enhancement of d^o_{24} and d^o_{15} near the transition points is directly related to the orthorhombic-tetragonal and orthorhombic-rhombohedral phase transitions, respectively, which involves a polarization rotation from the $[011]^c$ cubic ($[001]^o$ orthorhombic) axis toward the $[001]^c$ axis and from $[011]^c$ cubic ($[001]^o$ orthorhombic) axis toward the $[111]^c$ cubic axis. However, our calculating results show that the temperature dependence of the shear piezoelectric coefficients is significantly reduced by the electric field along the polar direction [Fig. 6(b)]. The temperature effects on the piezoelectric coefficients are diminished under the applied electric field. As a result, it is not easy to transform $KNbO_3$ crystal from the orthorhombic phase to either tetragonal or rhombohedral phase by changing the temperature. The result is consistent with the temperature-electric field phase diagram [Fig. 5(b)] that the transition temperatures for the orthorhombic-α and orthorhombic-β phase transition increase and decrease under an electric field, respectively.

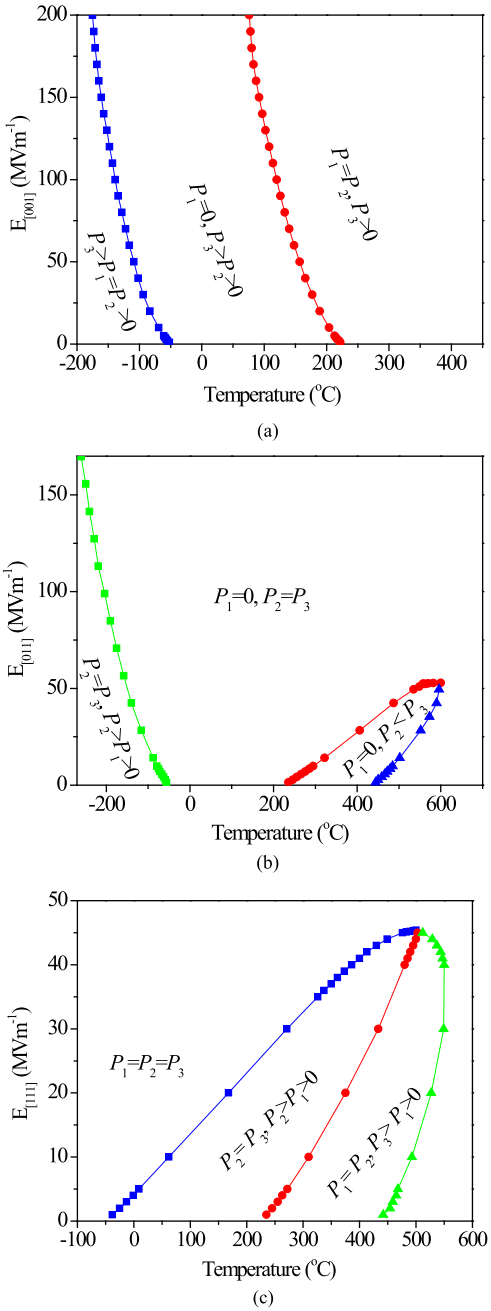

FIG. 5. Phase diagram as a function of temperature and applied electric field (a) $E = (0, 0, E_0)$ so that $E_{[001]^c} = E_0$; (b) $E = (0, E_0, E_0)$ so that $E_{[011]^c} = \sqrt{2}E_0$; (c) $E = (E_0, E_0, E_0)$ so that $E_{[111]^c} = \sqrt{3}E_0$.

Downloaded 13 Nov 2012 to 146.186.211.66. Redistribution subject to AIP license or copyright; see http://jap.aip.org/about/rights_and_permissions

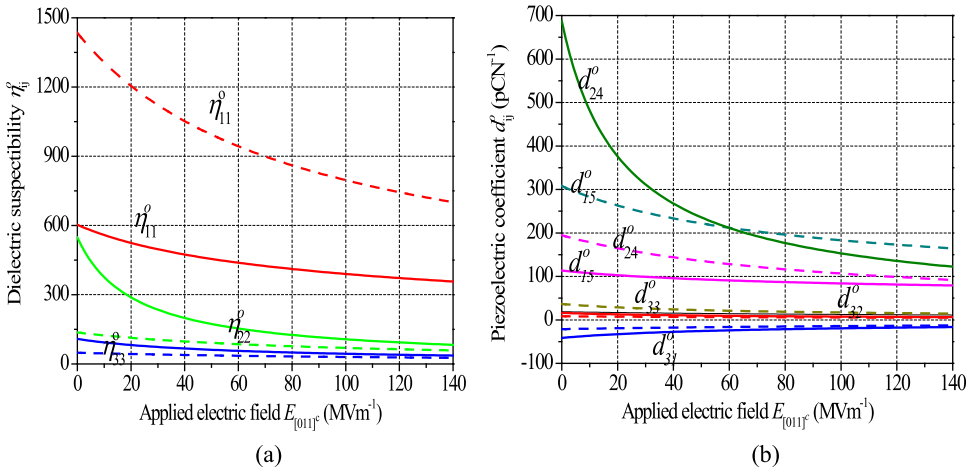

FIG. 6. Calculated electric field dependence of (a) the dielectric susceptibility η_{ij}^o and (b) the piezoelectric coefficients d_{ij}^o for single-domain $KNbO_3$ crystal at 200 °C (solid lines) and −45 °C (dashed lines).

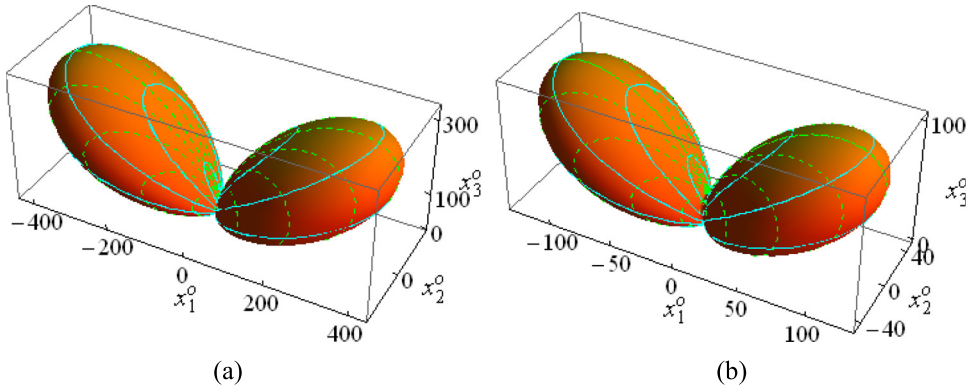

FIG. 7. The orientation dependence of the piezoelectric coefficient d_{33}^{o*} for two selected positive bias electric fields at 200 °C, (a) $E = 0$ MV/m; (b) $E = 35$ MV/m. The three coordinate axes correspond to $x_1^o = d_{33}^{o*}\sin\theta\cos\phi$, $x_2^o = d_{33}^{o*}\sin\theta\sin\phi$, $x_3^o = d_{33}^{o*}\cos\theta$, respectively. The numerical values marked on the axes have unit pC/N. The piezoelectric coefficients are symmetry with respective to the plane of $x_3^o = 0$, so only the upper half of the coordinate space is shown.

In order to illustrate the crystallographic orientation dependence of d_{33}^{o*}, the d_{33}^{o*} surface under the given electric fields of 0 and 35 MV/m at temperature 200 °C is plotted in Fig. 7. The angle corresponding to the maximum d_{33}^{o*} is nearly independent of the electric field.

Figure 8 shows the orientation dependence of piezoelectric coefficients $d_{33}^{o*}(\theta, \phi)$ [see Eq. (3)] under the electric fields of 0 and 35 MV/m at temperature 200 °C and −45 °C. At high temperature, the positive bias field decreases the maximum d_{33}^{o*} from 278.1 (without any electric field) to 120.1 pC/N for $\phi = 0°$. It can be easily seen from Eq. (3) that the decrease of d_{33}^{o*} along the $(100)^o$ plane is primarily due to the decrease of d_{24}^o. On the other hand, at −45 °C, the positive bias field reduces d_{33}^{o*} to 92.0 pC/N for $\phi = 90°$ which is larger than that at $\phi = 0°$(65.8 pC/N), implying that the maximum d_{33}^{o*} is along the $(010)^o$ plane. Compared with its value at higher temperature, d_{33}^{o*} is dominated by d_{15}^o in the lower temperature regime. It is consistent with the results of the shear piezoelectric coefficients d_{24}^o and d_{15}^o which are always larger than others at both high and low temperatures under any bias electric field. Thus, the piezoelectric responses are determined by the rotation direction of the polarization resulted by both temperature changes and external electric fields.

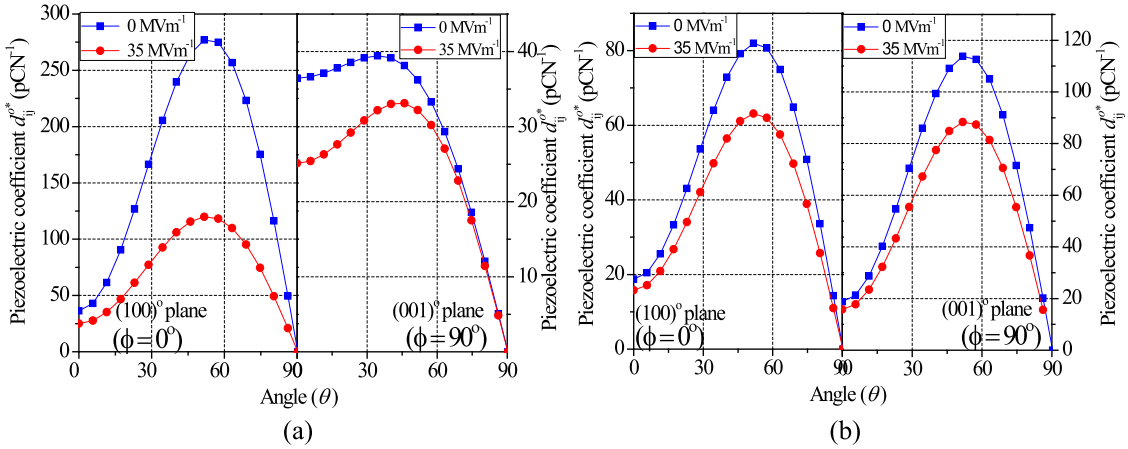

FIG. 8. Piezoelectric coefficient d_{33}^{o*} in the orthorhombic $KNbO_3$ as a function of angle θ under various applied electric fields $E_{[011]}c$ at temperature (a) 200 °C and (b) −45 °C. Only the piezoelectric coefficients in the angle θ between 0° and 90° are shown.

Downloaded 13 Nov 2012 to 146.186.211.66. Redistribution subject to AIP license or copyright; see http://jap.aip.org/about/rights_and_permissions

In summary, we have studied the effects of hydrostatic pressure and electric field ($E_{[011]c}$) on the piezoelectric responses of single-domain $KNbO_3$ single crystals using the Landau-Ginzburg-Devonshire thermodynamic theory. The effect of hydrostatic pressure on the piezoelectric response is very similar to that of temperature if we assume a ferroelectric phase transition is in the first-order. The phase diagram as a function of electric field and temperature is constructed based on the thermodynamic calculations. The applied electric fields parallel to the polar direction reduce the dielectric and piezoelectric responses of $KNbO_3$ crystals. The maximum of the piezoelectric coefficient d_{33}^{o*} is determined by the rotation of the polarization resulted by both temperatures and external electric fields. To further calculate the piezoelectric responses of $KNbO_3$ sintered ceramics under the applied external fields, we have to extend the current thermodynamic calculations to phase field simulations, in which the effect of polycrystal microstructures and multi-domains can be included.

The work is partially supported by NSF under ECCS-0708759 and DMR-1006541. The computer simulations were carried out on the LION and Cyberstar clusters at the Pennsylvania State University supported in part by NSF Major Research Instrumentation Program through Grant No. OCI-0821527.

[1]K. Yamanouchi, H. Odagawa, T. Kojima, and T. Matsumura, Electron. Lett. **33**, 193 (1997).
[2]G. Shirane, R. Newnham, and R. Pepinsky, Phys. Rev. **96**, 581 (1954).
[3]K. Nakamura, T. Tokiwa, and Y. Kawamura, J. Appl. Phys. **91**, 9272 (2002).
[4]S. Wada, A. Seike, and T. Tsurumi, Jpn. J. Appl. Phys. Part 1 **40**, 5690 (2001).
[5]J. Hirohashi, K. Yamada, H. Kamio, M. Uchida, and S. Shichijyo, J. Appl. Phys. **98**, 034107 (2005).
[6]S. Wada, K. Muraoka, H. Kakemoto, T. Tsurumi, and H. Kumagai, Jpn. J. Appl. Phys. Part 1 **43**, 6692 (2004).
[7]J. Kuwata, K. Uchino, and S. Nomura, Jpn. J. Appl. Phys. Part 1 **21**, 1298 (1982).
[8]S. E. Park and T. R. Shrout, J. Appl. Phys. **82**, 1804 (1997).
[9]X. Du, U. Belegundu, and K. Uchino, Jpn. J. Appl. Phys. Part 1 **36**, 5580 (1997).
[10]S. Wada, S. Suzuki, T. Noma, T. Suzuki, M. Osada, M. Kakihana, S.-E. Park, L. E. Cross, and T. R. Shrout, Jpn. J. Appl. Phys. Part 1 **38**, 5505 (1999).
[11]A. Garcia and D. Vanderbilt, Appl. Phys. Lett. **72**, 2981 (1998).
[12]L. Bellaiche, A. Garcia, and D. Vanderbilt, Phys. Rev. Lett. **84**, 5427 (2000).
[13]H. Fu and R. E. Cohen, Nature **403**, 281 (2000).
[14]M. Budimir, D. Damjanovic, and N. Setter, Phys. Rev. B **72**, 064107 (2005).
[15]M. Budimir, D. Damjanovic, and N. Setter, Phys. Rev. B **73**, 174106 (2006).
[16]M. J. Huan, E. Furman, S. J. Jang, H. A. Mckinstry, and L. E. Corss, J. Appl. Phys. **62**, 3331 (1987).
[17]D. Damjanovic, F. Brem, and N. Setter, Appl. Phys. Lett. **80**, 652 (2002).
[18]M. Budimir, D. Damjanovic, and N. Setter, Appl. Phys. Lett. **85**, 2890 (2004).
[19]D. Damjanovic, J. Am. Ceram. Soc. **88**, 2663 (2005).
[20]M. Budimir, D. Damjanovic, and N. Setter, J. Appl. Phys. **94**, 6753 (2003).
[21]S.-E. Park, S. Wada, L. E. Cross, and T. R. Shrout, J. Appl. Phys. **86**, 2746 (1999).
[22]E. Wiesendanger, Ferroelectrics **6**, 263 (1974).
[23]P. Günter, Jpn. J. Appl. Phys. Part 1 **16**, 1727 (1977).
[24]M. Zgonik, R. Schlesser, I. Biaggio, E. Voit, J. Tscheny, and P. Günter, J. Appl. Phys. **74**, 1287 (1993).
[25]A. G. Kalinichev, J. D. Bass, C. S. Zha, P. D. Han, and D. A. Payne, J. Appl. Phys. **74**, 6603 (1993).
[26]L. Liang, Y. L. Li, S. Y. Hu, L.-Q. Chen, and G.-H. Lu, J. Appl. Phys. **108**, 094111 (2010).
[27]L. Liang, Y. L. Li, L.-Q. Chen, S. Y. Hu, and G.-H. Lu, J. Appl. Phys. **106**, 104118 (2009).
[28]M. J. Haun, E. Furman, S. J. Jang, and L. E. Cross, Ferroelectrics **99**, 13 (1989).
[29]L. Liang, Y. L. Li, L.-Q. Chen, S. Y. Hu, and G.-H. Lu, Appl. Phys. Lett. **94**, 072904 (2009).

Downloaded 13 Nov 2012 to 146.186.211.66. Redistribution subject to AIP license or copyright; see http://jap.aip.org/about/rights_and_permissions